


ORIGINAL RESEARCH

Quantitative characteristics of the striking distance to wind turbine blades based on an improved stochastic lightning model

Xiaoyan Bian^{1,2} | Yong Wu¹  | Qibin Zhou³ | Ruijiao Jiang² | Yao Zhang⁴ |
Lyuwen Chen⁵ | Qi Qi² | Weitao Lyu²

¹School of Electrical Engineering, Shanghai University of Electric Power, Shanghai, China

²State Key Laboratory of Severe Weather, Chinese Academy of Meteorological Sciences, Beijing, China

³School of Mechatronic Engineering and Automation, Shanghai University, Shanghai, China

⁴Taizhou Power Supply Company, State Grid Zhejiang Electric Power Company, Taizhou, China

⁵Institute of Tropical and Marine Meteorology, China Meteorological Administration, Guangzhou, China

Correspondence

Qibin Zhou, School of Mechatronic Engineering and Automation, Shanghai University, Shanghai 200444, China.
Email: zhouqibin@shu.edu.cn

Funding information

National Key Research and Development Program of China, Grant/Award Number: 2017YFC1501504; Open Grants of the State Key Laboratory of Severe Weather, Grant/Award Number: 2021LASW-B06

Abstract

The damage of wind turbines suffered from lightning strikes has been a key issue for the safe and reliable operation of wind farms. Accurate determination of the annual lightning flash number to a wind turbine is essential for designing proper lightning protection measures. The interaction of downward and multiple upward leaders (MULs) is studied in this paper, which also considers the stochastic nature and branched behaviour of the lightning attachment phenomenon. Firstly, with an improved stochastic lightning model, the relationship among the striking distance, the height of wind turbines and the return stroke current is established. Moreover, a modified method for predicting the annual lightning flash number strikes to a wind turbine is proposed. The simulation results show that the striking distance and the collection area not only depend on the return stroke current, but also on the height and blade angle. Besides, the comparisons between the calculation results and field statistics indicate that the conventional electric geometry model is not satisfied with the need of lightning protection for wind turbines. Note that there is only a difference of 4% between the modified method and the observation value. These quantitative researches provide the guidance of calculation results for the optimization of the blade lightning protection system (LPS) design.

1 | INTRODUCTION

Wind energy, which accounts for a significant amount of the clean energy sources, has become an indispensable approach for addressing the climate change in worldwide [1]. But the flourishing development of wind power industry and the enlargement of the capacity and size goes with the lightning risk of lightning damage on wind turbines [2]. The huge economic losses and serious social impact caused by lightning strike accidents have severely affected the safety and reliability of wind farms. Therefore, it is an urgent need to carry out the researches on the evaluation of the lightning exposure assessment of wind turbines. As key parameters, the appropriate analysis of the lightning striking distance, the equivalent lightning collection area and the annual lightning flashes striking to a wind turbine

are of great significance to lightning protection of wind turbines.

Nowadays, the lightning protection of the structure has been carried out widely by employing the classical Electrical Geometry Model (EGM) improved by Love and Eriksson [3, 4]. However, the modification of the EGM-striking distance, as the core of EGM, depends on the observation data. The disadvantages of vague concept and poor universality result in a large difference between the calculation result and the fact. Cooray et al. [5], based on the self-consistent leader inception and propagation model (SILM), took the presence of a connecting leader into account and deduced the striking distance equation of buildings for different heights. Nevertheless, the competitive effect of multiple upward leaders (MULs) and stochastic nature cannot be ignored [6, 7].

This is an open access article under the terms of the [Creative Commons Attribution-NonCommercial-NoDerivs](https://creativecommons.org/licenses/by-nc-nd/4.0/) License, which permits use and distribution in any medium, provided the original work is properly cited, the use is non-commercial and no modifications or adaptations are made.

© 2023 The Authors. *IET Generation, Transmission & Distribution* published by John Wiley & Sons Ltd on behalf of The Institution of Engineering and Technology.

The lightning striking distance to the ground (R_s) is a vital parameter to represent the attracting ability of the ground to downward leader. Nevertheless, the previous equation for striking distance to the ground obtained in [8–10] did not consider the influence of the objects on the ground electric field. IEEE Std 1243-1997 [11] gave the recommended equation for striking distance to the ground. Since it was proposed in the context of transmission lines, its applicability to the situation of wind turbines should be further analyzed. At present, there is a lack of a suitable equation for the striking distance to the ground in the presence of wind turbines.

Peesapati et al. [12] made a statistical analysis for the frequency of lightning incidences in the wind farm of Denmark during a period of 3 years, and found that the actual number suffered by wind farms was quite different from the calculated using Eriksson model, which demonstrates that the lightning protection standards adopted widely by wind turbines are seriously inaccurate. Observe that the estimations of the annual number suffered by wind farms based on the lightning flash density reported before the turbines were installed, neglect the fact that wind turbines have a higher probability to be struck by lightning compared with their surroundings [13]. The actual lightning flash density to a wind park area is likely to increase compared with the historical values reported before the turbines were installed. Up to now, the stochastic nature of the lightning attachment phenomenon is usually neglected on the existing analysis of lightning interception and shielding failures estimation. But, in fact, the inherent random characteristic of propagation plays a great role in the background potential configuration and the final lightning attachment process [14]. Additionally, it is well known that structures higher than 100 m, such as high wind turbines, experience a higher electric field enhancement during a thunderstorm that may cause longer upward connecting leaders (UCLs). For a given return stroke current, its length increases with increasing height of the structure, and the actual striking distance also increases as the height of the structure is increased [5]. Therefore, the accuracy of evaluating the lightning striking performance of wind turbine blades with the traditional EGM is questionable. That is, it is indispensable to introduce an improved calculation method.

Currently, numerical simulation has progressively captured scholars' attention as a substantial means to explore the characteristics of lightning strike in that it is economical and efficient, which can control the parameters of the study and conduct a host of simulation tests. The stochastic lightning model was used by Jiang et al. in [15] to simulate cloud-to-ground lightning strikes to structures. Furthermore, Guo et al. [16] had carried out three-dimensional (3D) modelling, which took into account the true geometry of the lightning channel and the earthed structures involved in the lightning attachment process. But the simulation space of the research was set in a much smaller space for a less demand on computer memories and CPU resources, and they do not consider the speed ratio of downward leader to upward leader and the lightning current amplitude. So, there are many regrets in the 3D model.

In this paper, an improved Stochastic Leader Model (SLM) is performed to provide the guidance to the lightning protection for the wind turbine, which focuses on the interaction of downward and MULs. The proposed model takes into account all the stochastic nature of the lightning attachment phenomenon, the lightning discharge branched and tortuous behaviour. By adjusting the parameters, the relationship among the striking distance, the height of the wind turbine and the prospective return stroke current is discussed. And considering the existence of the wind turbine, the equation for lightning striking distance to ground and the striking distance coefficient are researched and modified. Then, combined with the traditional EGM, the calculation model of equivalent lightning collection area and the annual number of lightning strikes to a wind turbine is improved, and the statistical results are in agreement with factual observation data. Moreover, the corresponding lightning protection levels (LPLs) adopted by different methods are discussed.

2 | NUMERICAL MODEL

Comparing with the single-leader model, the initiation of MULs and the electric field algorithm are optimized in the model of multiple leaders. Based on the research of Jiang et al. [15] and Tan et al. [17], this work further adjusts the simulation area and discharge parameters, so as to realize the simulation of the real lightning attachment process.

2.1 | Two-dimensional stochastic leader model

2.1.1 | Initiation of multiple upward leaders

In this study, as long as the grid point meets the trigger threshold (500 kV/m), it can incept upward positive leader (UPL). Thereby, during the descent of the downward negative leader (DNL), it is imperative to update the spatial potential distribution and search again for the initial point of the UPL in the simulation area at each new step of the DNL. Diverse MULs can be initiated at different development steps of DNL, or simultaneously can be initiated at a certain step. When multiple grid points reach the criterion of initiating upward leader at the same time, the grid point of the maximum electric field is selected to start the UPL first.

2.1.2 | Development and connection of leaders

Given the optical observations, it has been found that DNL can produce multitudes of branches, but UPL rarely bifurcate [18]. During the propagation of leaders, each developed grid point of DNL can extend to the surrounding undeveloped points, while for the UPL only the grid points on the head can extend to the surrounding undeveloped points, as illustrated in Figure 1. In addition, under the condition of multiple

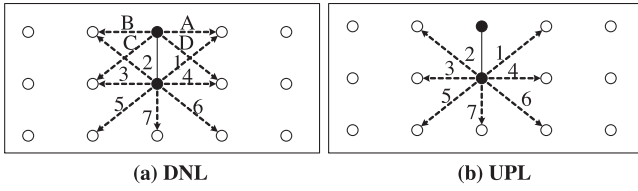


FIGURE 1 Schematic diagram of the development possibilities (the solid dots are the developed steps, the hollow dots are the undeveloped steps, and the arrows are the possible development paths). (a) The negative leader, (b) the positive leader.

leaders, the DNL and the UPL develop cyclically and contemporaneously. At the end of each cycle, the electric field value between the head point of the DNL and all channel points of the UPL is calculated to determine whether the final jump will occur.

The next jump of the leader after each step is almost chosen randomly in the space among all possible new extensions for which electric field values reach the given thresholds (220 kV/m) beneath the leader tip; the probability of determining the subsequent channel point is given as follows [19]:

$$P_{i'} = \begin{cases} \frac{(E_{i'} - E_{cr})^\eta}{\sum_{j=1}^N (E_{i_j} - E_{cr})^\eta}, & E_{i'} \geq E_{cr} \\ 0, & E_{i'} < E_{cr} \end{cases} \quad (1)$$

where i' is the leader tip point, i is the surrounding points near i' , $P_{i'}$ is the probability of potential point i to be selected as the next jump, N is the total number of potential points, $E_{i'}$ the electric field intensity in the space from i to i' , E_{cr} (kV/m) is the critical electric field required for discharge propagation, η is the developing probability index whose value is 1 in the subsequent simulation.

2.1.3 | Computation of the spatial electric field

The electric field spatial distribution around the lightning channel will influence the charges in the lightning channel. After each new extension, the electric potentials φ at grid points not on the channel must be updated by solving Poisson's equation, which is shown as Equation (2). The electric potential at every point of the 2-D domain is computed by iteratively solving the Laplace equation adopting the finite difference method (FDM) by combining with the successive over-relaxation technique (SOR) utilizing MATLAB. Then, the iterative formula of the potential φ at any discrete point (i, j) in the model area is shown in Equation (3):

$$\nabla^2 \varphi = -\frac{\rho}{\varepsilon} \quad (2)$$

$$\varphi_{i,j}^{n+1} = \varphi_{i,j}^n + \frac{\omega}{4} \times (\varphi_{i+1,j}^n + \varphi_{i,j+1}^n + \varphi_{i-1,j}^{n+1} + \varphi_{i,j-1}^{n+1} - 4\varphi_{i,j}^n) \quad (3)$$

where φ is the electric potential; ρ is the net charge density at points not on the channel; ε is the dielectric constant of air; ω is the overrelaxation parameter, ω is 1.975 in this study.

2.2 | Main parameters in the model

In this paper, to minimize the effects of air boundaries, a 5000 m \times 1500 m two-dimensional simulation domain near-surface ground is constructed. Moreover, the environmental electric field is evenly distributed, the downward leader is the negative leader and the upward leader is the positive leader. Then the spatial background electric field intensity increases from bottom to top within the range of 1500 m above the ground. Besides, the potential of the ground and the wind turbines are set at 0 V. Given the corona produced by the tips of wind turbines, the electric field intensity of the lower boundary is -5 kV/m and the upper boundary is -90 kV/m [15]. Assuming that the ground, DNL and wind turbines are set at zero potential (Dirichlet boundary condition). The air boundary of the simulation domain satisfies Neumann boundary conditions ($\partial\varphi/\partial n = 0$).

Meanwhile, the leader channel is assumed to be completely ionized and there is a DNL which has a length of 40 m and is set with a certain electric potential V_0 . The initial position of DNL is fixed at the uppermost of the simulation area. The electric potential at the downward leader tip V_0 (V) is given as a function of the lightning peak current I_p (kA) by the following equation proposed by Cooray [5]:

$$V_0 = 3 \times 10^6 I_p^{0.813} \quad (4)$$

As this work only simulates the near-ground part of DNL, so the initiation of DNL is not involved. In general, the initiation threshold of leader is larger than its propagation threshold [20]. This model also set the propagation threshold of the DNL and UPL as 220 kV/m which adopts trigger threshold for UPL of 500 kV/m. The critical breakdown electric field is thought of as 500 kV/m [21, 22]. According to previous studies, the speed ratio of UPL and DNL is confirmed as 1:4 [23]. In practice, the choice of discharge parameters is somewhat subjective, in view of the uncertainty of the charge distribution in the channel and space and other factors in the actual discharge process. But the values above are reasonable in accordance with the previous research.

The selected key model parameters are concluded in Table 1 and Figure 2 is the flow diagram of the model for multiple leader development.

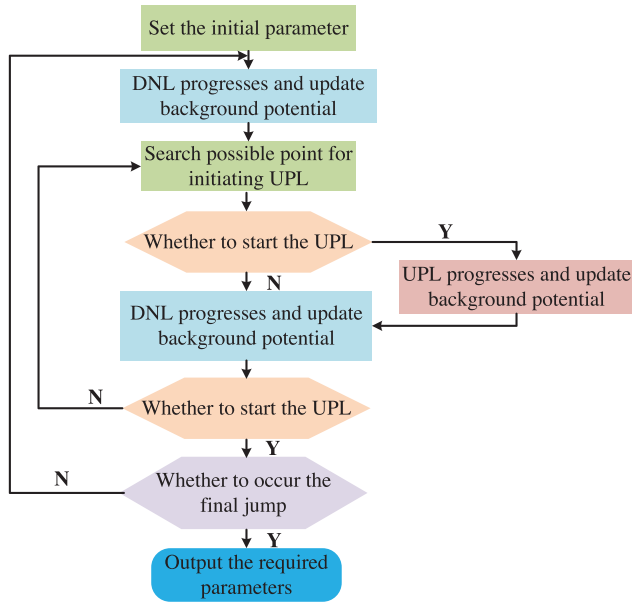
2.3 | Design of simulation for various scenarios

Figure 3 is a schematic diagram of the simulation area. The previous research results indicated that the blade is relatively still during the attachment process [24]. To simplify the descrip-

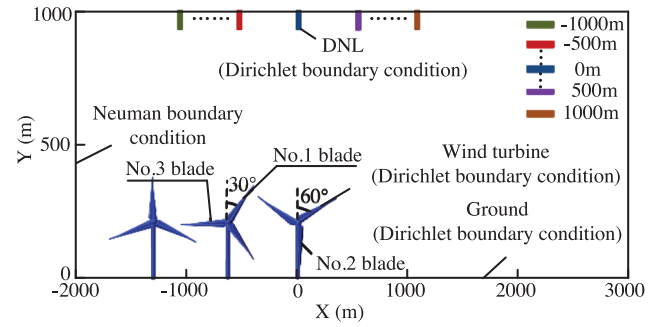
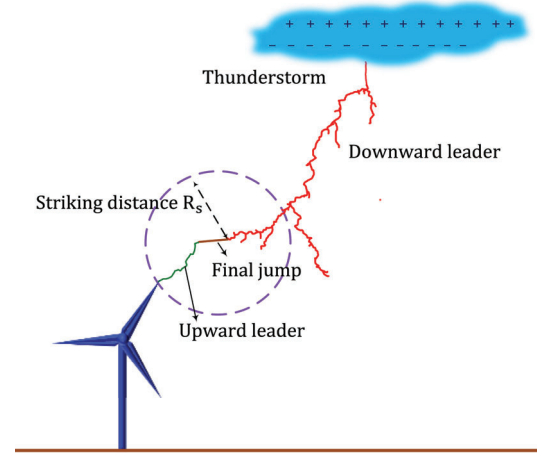
TABLE 1 Model parameters

Model parameters	Values
Simulation area	5000 m × 1500 m
Field strength at the ground-level	−5 kV/m
Field strength at the top boundary	−90 kV/m
Propagation parameter η	1
Critical electric field E_{cr} (DNL and UPL)	220 kV/m
Initiation threshold (UPL)	500 kV/m
Initial length (DNL)	40 m
Developed probability formula	Equation (1)
The final attachment threshold	500 kV/m
The speed ratio of DNL to UPL	4:1
The electric potential at the DNL tip	Equation (3)

DNL, downward negative leader; UPL, upward positive leader.

**FIGURE 2** Flow diagram of the model for multiple leader development.

tion below, the blade in the first quadrant is named as No. 1 blade, the other two as No. 2 and No. 3 blade in the clockwise direction, respectively. The wind turbines are conducted under three basic states according to the rotation angle of the No. 1 blade, which are 0° , 30° and 60° , as shown in Figure 3. The blade angle θ is the angle between the No.1 blade and the vertical direction with the clockwise direction being positive. The wind turbine is fixed on the site of the abscissa of 0 with diverse heights, and rectangles in various colours represent different initial positions of DNL. The abscissa of the DNL initial position is regarded as the lateral distance which ranges from −1000 to 1000 m (The negative value indicates that the initial position of the DNL is on the left of the wind turbine, and the positive value indicates that it is on the right, also with an interval of 100 m).

**FIGURE 3** Spatial schematic diagram of the simulations.**FIGURE 4** Schematic diagram of the striking distance.

The actual process of lightning strikes to a wind turbine is not the process of lightning directly attachment to the wind turbine, but the connection of UPL and DNL initiated from the wind turbine. That is, the accuracy of evaluating the lightning striking performance with the traditional concept of striking distance is questionable. In this research, based on the SLM, the distance between the point of the wind turbine, where a connecting leader is initiated, and the heads of DNL when the final jump condition is established between the connecting leader and the DNL, is defined as striking distance (as shown in Figure 4). Firstly, the striking distance changes with different blade angles and tower heights, and it not only can clarify the physical meaning of the striking distance in a conventional EGM but can also adapt to the complex mechanical structure and rotating characteristics of turbine blades.

The Monte Carlo method can consider well the randomness of a lightning stroke and obtain reasonable results. While for the lightning attachment process, it is necessary to run an extremely large number of cases to ensure evaluation accuracy. The Monte Carlo method has been used for analysis of lightning strikes widely [25–28]. In fact, simulations of the lightning phenomenon using SLM proposed in this paper can be identified as the Monte Carlo method. It shows the complex process of lightning strike that essentially involves many aspects of randomness. And the calculation of striking distance should

involve Monte Carlo methods during simulation. The factors that determine the value of striking distance are the initial position of DNL, the blade rotation angle, the height of wind turbines and the lightning peak current. However, the parameters of the blade rotation angle, the initial position of DNL and the lightning peak current are stochastic. In Monte Carlo simulation, analysis is carried out for a large number of lightning strokes. Each process is repeated at least 400 times with random values of every selected parameter to obtain random lightning stroke samples. For each lightning stroke, striking distance is calculated using the above concept. Therefore, while simulating a model of strikes that includes these random properties of the lightning process, the initial position of DNL, the blade rotation angle, the height of wind turbines and the lightning peak current have to be suitably chosen stochastic variables.

According to the Monte Carlo idea, the striking distance should be derived from a large number of simulation tests. Therefore, the cases of lightning flashes with various return stroke current striking to the different heights of wind turbines are simulated to highlight the randomness. In diverse cases, 400 simulation tests are performed for each lateral distance (from -1000 to 1000 m). There are in total 8000 simulation results for each case. The value of the striking distance for each case is the arithmetic mean of the simulation results when the lightning strikes to the wind turbine blade.

3 | QUANTITATIVE CHARACTERISTICS OF THE STRIKING DISTANCE

3.1 | Exploration of the striking distance

The most common case is that the striking point is at the tip of the wind turbine blades. The tip of the DNL connects to the lateral of the UCL in Figure 5a, and the tip of the DNL connects to the tip of the UCL in Figure 5b, which is consistent with the observation in Lu et al. [29] by the high-speed video camera, as shown in Figures 5c and 5d. Also, similar to the observations from the Rakov group [30] and the Qie group [31], the simulated discharge channel propagates in a zig-zag manner and produces extensive branches.

In this section, the simulation results of a typical wind turbine of 160 m are analysed, where the height of the tower and the length of the blade are, respectively, 110 and 50 m. This work shows the lightning exposure arcs of the tip points under the different lightning current with the rotor orientations from 0° to 60° . As shown in Figures 6a and 6c, the striking distances of No. 1 blade and No. 3 blade are roughly the same at blade angles of 0° and 60° , which are in symmetrical states. Then, it can be seen from Figure 6b that the striking distance of No. 3 blade is much smaller than that of No.1 blade at a blade angle of 30° . This is because there is a shielding effect among the blades. Additionally, the striking distance of wind turbine blades is 0° , 30° and 60° from large to small, the main reason for this being that the effective height of the wind turbine decreases as

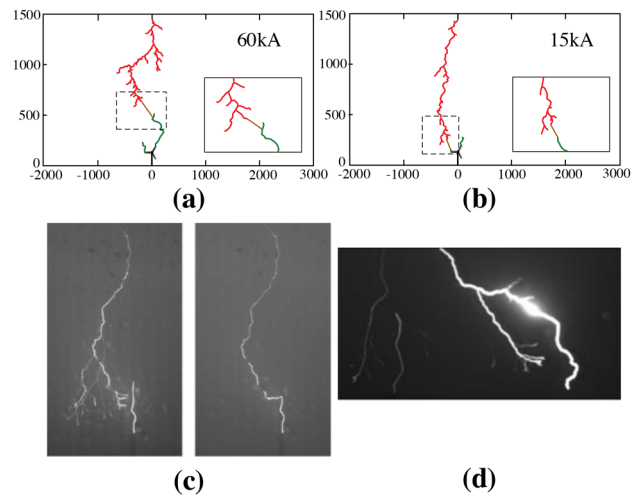


FIGURE 5 Simulation results. (a) A flash strikes the top of the wind turbine with a tip-to-lateral attachment. (b) A flash strikes the top of the wind turbine with a tip-to-tip attachment. (c) The high-speed images (tip-to-lateral attachment). (d) Tip-to-tip attachment.

the blade angle increases, and the distortion effect on the background electric field will be weakened which leads to a smaller electric field value. Thus, the DNL needs to be closer to the wind turbine to trigger the UPL.

The traditional striking distance equation has been widely used in the lightning protection of transmission line and lightning rods. The wind turbine blade can be roughly thought of as a lightning rod when $\theta = 0^\circ$. Thereby, the traditional striking distance equation can be used to calculate the striking distance of wind turbine blades, which is an appropriate application of the conventional method, when the blade is vertically upward.

As shown in Figure 6d, here, the values are the arithmetic mean of the simulation results for each I_p , and according to the striking distance equation of Reference [5], the curve fitted to these data is expressed as

$$R_s = 12.452 I_p^{0.855} \quad (5)$$

where R_s (m) is the striking distance of wind turbine blades and I_p (kA) is the prospective return stroke current.

The results derived from this paper are compared with other calculation methods, for example Petrov and Waters [32], Eriksson [33], Cooray et al. [5] and the IEC standard [34]. Observe in Figure 6d that the R_s increases with the increasing I_p , but the R_s derived from this paper is larger than the values assumed in the other methods for lightning current exceeding 40 kA. For a smaller I_p the results calculated in this paper are between the equation of the Petrov and Eriksson. It should be pointed out that the previous equation of the striking distance without the impact

of the interaction of DNL and MULs, the final attachment process or the stochastic nature of the lightning attachment phenomenon, which will weaken the effect of the structure on lightning.

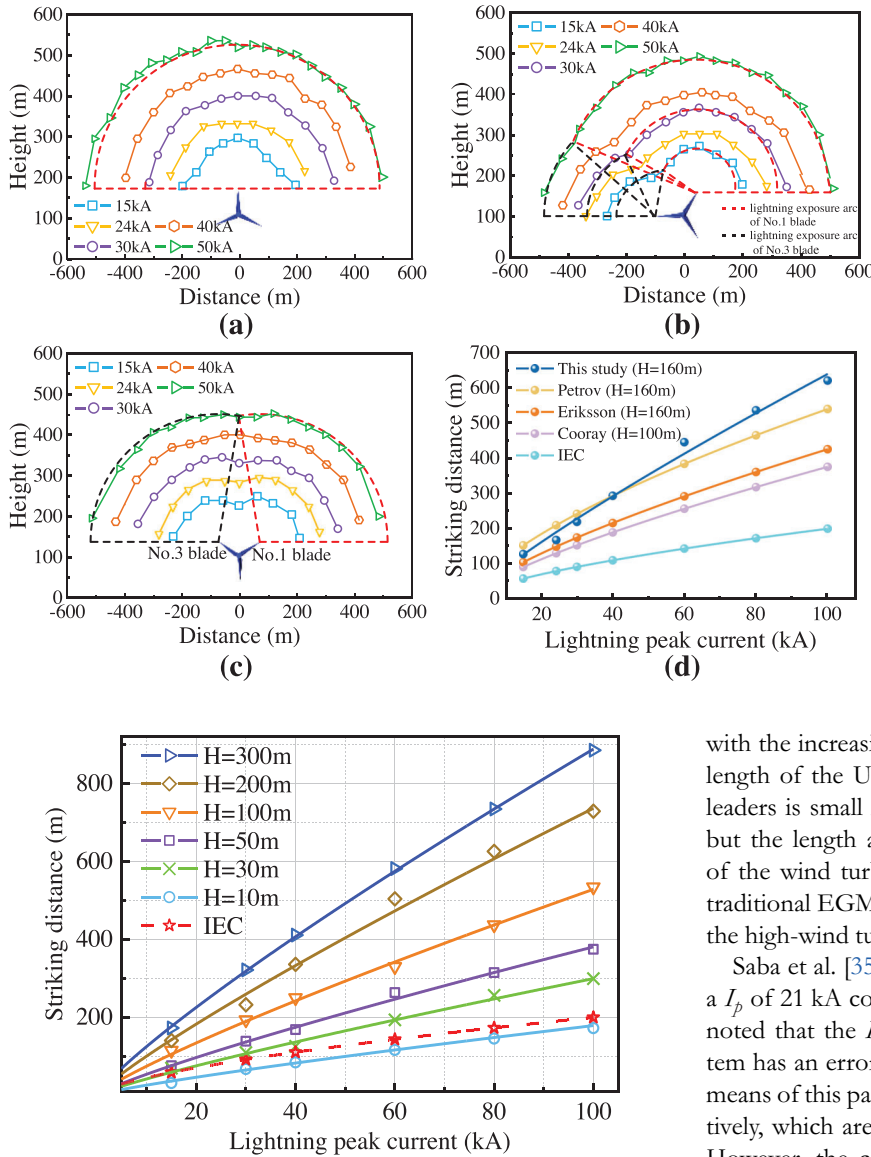


FIGURE 6 Simulation results of the striking distance for a 160-m high wind turbine. (a) Lightning exposure arc of the wind turbine blade when $\theta = 0^\circ$, (b) $\theta = 30^\circ$, (c) $\theta = 60^\circ$, (d) the striking distance of different return stroke currents evaluated from the different model.

FIGURE 7 The relationship among the striking distance, the height of the wind turbine and the prospective return stroke current.

Furthermore, the higher the wind turbine is that may cause longer UCLs for a given I_p . Thus, the actual striking distance increases as the height of the wind turbine (H) is increased. On the contrary, the IEC striking distance does not vary with the H because it depends only on the I_p . For this, we have conducted research on the relationship among the R_s , H and I_p . From Figure 7, the relationship can be fitted as follows:

$$R_s = 1.178 H^{0.473} I_p^{0.853} \quad (6)$$

where H is the effective height of the wind turbine when $\theta = 0^\circ$, the coefficient of determination of Equation (6) is 0.994 ($R^2 = 0.994$).

According to Figure 7, for a small H , the difference between the IEC striking distance and the striking distance in this work is not evident, but the error using the IEC equation increases

with the increasing height. The reason for this trend is that the length of the UPL and the degree of stochastic behaviour of leaders is small in the case of low wind turbines or a small I_p , but the length and the degree increase with the rising height of the wind turbine and lightning current. That is to say, the traditional EGM is not satisfied with the need of protection for the high-wind turbines or large lightning current.

Saba et al. [35] observed that a 52-m high lightning rod with a I_p of 21 kA corresponds to a striking distance of 120 m. It is noted that the I_p obtained by the local lightning location system has an error of 10 kA. The calculated striking distances by means of this paper are 102 and 143 m of 21 and 31 kA, respectively, which are in good agreement with the observed results. However, the calculation results given by the different traditional striking distance models would vary from a minimum of 58 m to a maximum of 94 m for this event.

In a word, there will be some errors between the traditional striking distance and the truth. So, it is difficult to apply it in the complex rotating structure of wind turbines. The new equation for striking distance derived from this paper is in good agreement with actual situation compared with the IEC formula, which could provide a more physically realistic basis for lightning protection analysis.

3.2 | The striking distance to the ground in the presence of wind turbines

Considering that the UPL initiated from the wind turbine will distort the electric field on the ground, and it further affects the lightning striking distance to the ground (R_g). The traditional equation of the R_g is not applicable to the lightning protection calculation of the wind turbine. Therefore, it is necessary to discuss the R_g in the presence of wind turbines.

TABLE 2 Lightning striking distance to the ground and the striking distance coefficients

H/m	Striking distance/m	Return stroke current /kA				
		15	30	60	80	100
110 m	R_s	108	187	396	475	540
	R_g	47	83	166	206	239
	K	0.43	0.44	0.42	0.43	0.44
160 m	R_s	127	219	445	535	632
	R_g	47	84	165	205	238
	K	0.37	0.38	0.37	0.38	0.38
200 m	R_s	140	242	494	648	729
	R_g	45	81	168	205	244
	K	0.32	0.33	0.34	0.32	0.33

For a given return stroke current and a given wind turbine, the lateral distance (from -1000 to 1000 m) is changed by employing the model presented in this paper, and then each lateral distance is simulated 400 times. If for a lateral distance, there are about 50% of the simulation results that the final attachment is taken place between the DNL and the wind turbine. The lateral distance can be regarded as the point, where the probabilities of the lightning discharge to the ground and to the wind turbine are equal under the given case. After that, the arithmetic mean value of the lightning striking distance to the ground at this lateral distance is calculated, and the arithmetic mean value is R_g for the given current and the given wind turbine.

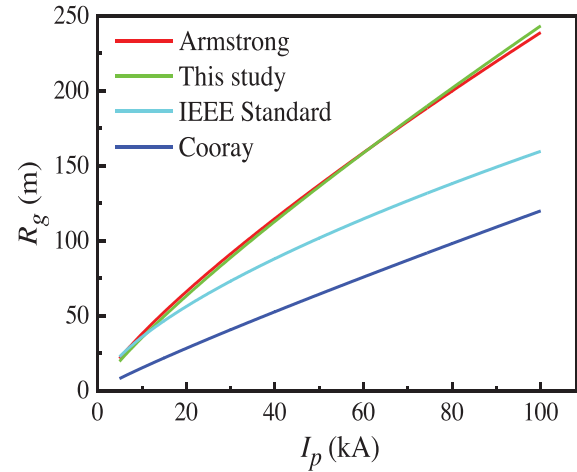
In the EGM, the striking distance coefficient K (the ratio of the lightning striking distance to the ground and striking distance to the conductor) is proposed to describe the difference of striking electric intensity between lightning leader to phase conductor and the ground. The ratio of striking distance to the ground and striking distance to the wind turbine blade derived from this paper can correspond to K , namely $K = R_g / R_s|_{p=50\%}$.

From the data in Table 2, it can be seen that R_g and R_s increase with the rising amplitude of I_p , but it basically has no effect on K ; The $K < 0.5$, and K will gradually decrease with the increase of H , which means that as H is risen, the difference of striking electric intensity between the lightning leader to the ground and the wind turbine will progressively increase. The relation between the striking distance coefficient K and the height of wind turbines H is

$$K = 0.56 - H/833 \quad (7)$$

The striking distance coefficient of transmission lines calculated by the given equation in the IEEE Std 1243-1997 [11] is 0.55 when the height is greater than 40 m, which is smaller than the results derived from this paper. Compared with the transmission lines, the wind turbine has a greater impact on the striking electric intensity for the ground.

The equation of the R_g proposed by previous scholars [8–10] is compared with the results derived from this paper in Figure 8.

**FIGURE 8** The R_g of different prospective return stroke currents evaluated from the different model.

And referring to the above-mentioned equation, the results from this paper are fitted as

$$R_g = 4.9I_p^{0.85} \quad (8)$$

where R_g is the lightning striking distance to the ground, I_p (kA) is the prospective return stroke current.

As illustrated in Figure 8, for a given I_p , the R_g calculated by this paper is consistent with the results obtained by Armstrong, and the results derived from other scholars are more conservative. Moreover, for the larger results attained in this paper, it demonstrates that the UPL initiated from the wind turbine can enhance the distortion degree of the electric field near the wind turbine at a certain lateral distance of DNL. Meanwhile, since the previous equation of the striking distance is based on the background of transmission lines, the conclusions do not fully represent the larger distortion degree of the wind turbine to the electric field in the nearby space.

4 | A MODIFIED CALCULATION METHOD OF THE ANNUAL LIGHTNING FLASH NUMBER

Lightning risk assessment for wind turbines should be based on the frequency of lightning strikes. Given that the precision and reliability of the existing method is insufficient, a more accurate calculation method of equivalent lightning attraction area and annual lightning flashes striking to a wind turbine is proposed in this paper.

4.1 | The structural model of a wind turbine

As shown in Figure 9, the three blades of the wind turbine are constantly rotating during its operation, and the effective height and the width of the wind turbine change as it rotates in

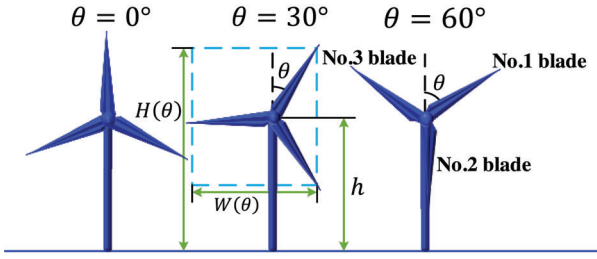


FIGURE 9 The structural model of a wind turbine.

the wind. And the width W for the first width variation cycle between $\theta = 0^\circ$ and $\theta = 60^\circ$, and the height H can be expressed as

$$W(\theta) = l \left(\sin(\theta) + \cos\left(\frac{\pi}{6} - \theta\right) \right) \quad (9)$$

$$H(\theta) = b + l \cos(\theta) \quad (10)$$

where l is the length of the wind turbine blade and θ is the angle between No. 1 blade and the Y -axis, b is the height of the wind turbine hub.

4.2 | The calculation method

The calculation diagram of the attractive radius by the EGM is shown in Figure 10, and the equation can be expressed as

$$\begin{cases} R_a = \sqrt{R_s^2 - (R_g - H)^2} & H \leq R_g \\ R_a = R_s & H > R_g \end{cases} \quad (11)$$

where R_s is the striking distance of different wind turbine blades calculated in Section 3.1, R_g is the striking distance to the ground calculated in Section 3.2.

Substituting (8) into (11) yields

$$\begin{cases} R_a = \sqrt{R_s^2 - \left(4.9I_p^{0.85} - H(\theta)\right)^2} & I > I_B \\ R_a = R_s & I \leq I_B \end{cases} \quad (12)$$

where I_B is the boundary current and given by

$$I_B(\theta) = e^{\ln((H(\theta)/4.9)/0.85)} \quad (13)$$

Then, the equivalent lightning collection area demonstrates that the number of lightning strikes in a certain area is the same as the number of lightning strikes intercepted by objects. As represented in Figure 11a, the equivalent collection area of the wind turbine with symmetrical wind turbine blades can be expressed as

$$A_e = \pi R_a^2 + 2R_a W(\theta) \quad (14)$$

As illustrated in Figure 11b, in the case of asymmetry, the collection area is

$$A_e = 0.5\pi \left(R_{a1}^2 + R_{a2}^2 \right) + (R_{a1} + R_{a2}) W(\theta) \quad (15)$$

where R_{a1} and R_{a2} are the attractive radii obtained from the striking distance of No. 1 and No. 3 blade, respectively.

Therefore, the annual number of lightning strikes to a wind turbine, N_d (times year⁻¹) can be expressed as

$$N_d = N_g \int_0^{2\pi} \int_0^\infty A_e(I_p, \theta) f(I_p) P_\theta dI_p d\theta \quad (16)$$

where N_g (km²year⁻¹) represents the ground flash density at the location of a wind turbine, $A_e(I_p, \theta)$ (km²) is the lightning collection area of a wind turbine under the I_p and the θ . In this study, the average value of the collection area (A_e) under the three conditions of blade angles of 0°, 30° and 60° is chosen as the collection area of a wind turbine for a given lightning current ($A_e(I_p)$ (km²)). P_θ is the probability density function of θ , and observe that the blade rotates at a uniform speed and θ may assume any value between 0 and 2π with equal probability when a lightning strike occurs, the angle probability density function is given by

$$P_\theta = \frac{1}{2\pi} \quad (17)$$

where $f(I_p)$ is the probability density function of I_p . According to IEC 62305-1 [34], the probability density of the stroke current I_p can be expressed as a lognormal distribution function of mean value μ and standard deviation σ_{log}

$$f(I_p) = \frac{1}{\left(I_p \cdot \sigma_{log} \cdot \sqrt{2\pi}\right)} \cdot \exp\left[-\frac{1}{2} \left(\frac{\ln(I_p) - \ln(\mu)}{\sigma_{log}}\right)^2\right] \quad (18)$$

where μ is 33.3 and σ_{log} is 0.263 in terms of IEC 62305 standard. So, the equivalent collection area of a given wind turbine A_{eq} is

$$A_{eq} = \int_0^\infty A_e(I_p) f(I_p) dI_p \quad (19)$$

Substituting (17), (18) and (19) into (16) simplifies

$$N_d = N_g \int_0^\infty A_e(I_p) f(I_p) dI_p \quad (20)$$

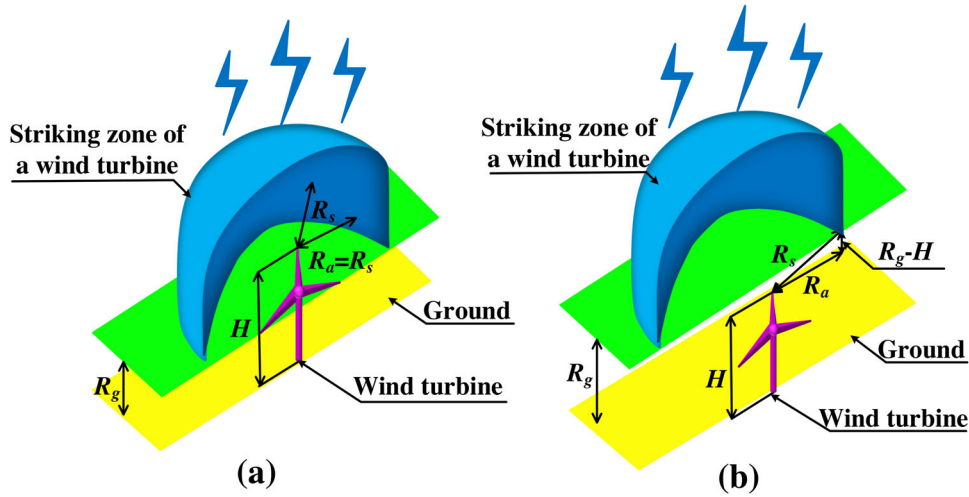


FIGURE 10 The calculation diagram of the attractive radius, R_a (a) $H > R_g$, (b) $H \leq R_g$.

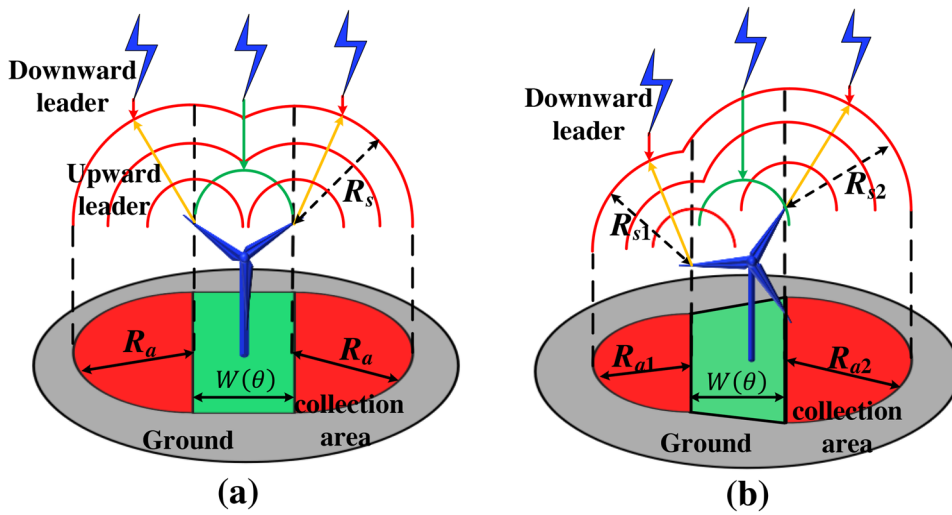


FIGURE 11 The lightning collection area, A_e , of a wind turbine (a) symmetrical state, (b) asymmetrical state.

4.3 | Results and analyses

4.3.1 | Discussion of the equivalent collection area

According to the literature, the I_p for negative ground flash measured by iron tower on Mont San Salvatore at an altitude of 915 m is 30 kA, and only 5% of the I_p exceeds 80 kA [12]. Meanwhile, some other studies also pointed out that the first return stroke has an average peak current of 30 kA [36]. Therefore, based on these observations, the value of I_p in the simulation is set as 15, 30 and 60 kA, respectively, and three typical kinds of wind turbines are mainly researched (110, 160, 200 m).

The schematic diagram of A_e predicted by this paper and EGM are compared as performed in Figure 12. The A_e of the nacelle is neglected, since it can be determined that its net contribution to the overall equivalent area is insignificant.

It can be known from Table 3 that the results derived from the IEC 61400-24 [37] remain the same no matter what state it is in, as it assumes the attractive radius is three times the height of the wind turbine without consideration of I_p and θ . The effective height of a wind turbine is 90 m for $H = 110$ m when $\theta = 60^\circ$ at l of 70 m and b of 40 m, and the A_e calculated by IEC 61400-24 is 229,022 m², which is 33% difference smaller than $\theta = 0^\circ$ (342,119 m²). This difference rises as the overall height of the wind turbine is increased. Consequently, the change of the effective height of a wind turbine must be taken into account while calculating A_e . Also, for a given I_p , the R_s predicted by IEC 62305-1 [34] does not vary with the structure height, and evidently, the A_e evaluated by it does not conform to the objective fact.

Table 4 presents the results of A_e derived from the calculation method in this paper. The A_e increases gradually with the increasing I_p for a given θ , which is in accordance with the

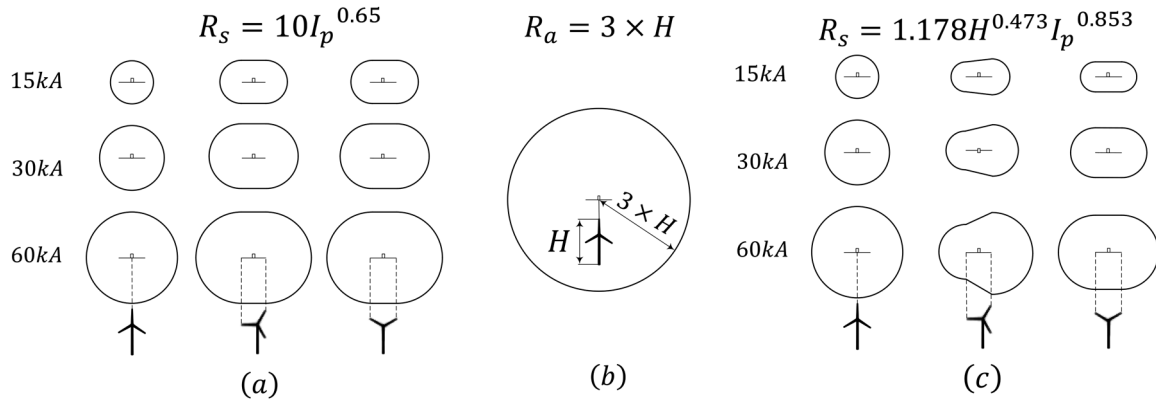


FIGURE 12 The schematic diagram of A_e evaluated from the various models (a) IEC 62305-1, (b) IEC 61400-24, (c) in this study.

TABLE 3 The equivalent collection area predicted by the two methods from the IEC standard

		IEC 62305-1 ($R_s = 10I_p^{0.65}$ EGM)			
		Blade angle of the wind turbine			
H/m	Return stroke current/kA :	0°	30°	60°	IEC 61400-24 $R_a = 3 * H$
110 m $(l = 70 \text{ m}, b = 40 \text{ m})$	$I_p = 15 \text{ kA}$	10,619 m ²	17,887 m ²	18,674 m ²	342,119 m ²
	$I_p = 30 \text{ kA}$	26,147 m ²	37,095 m ²	38,788 m ²	
	$I_p = 60 \text{ kA}$	64,377 m ²	81,555 m ²	84,212 m ²	
160 m $(l = 110 \text{ m}, b = 50 \text{ m})$	$I_p = 15 \text{ kA}$	10,619 m ²	19,340 m ²	20,689 m ²	723,822 m ²
	$I_p = 30 \text{ kA}$	26,147 m ²	39,837 m ²	41,948 m ²	
	$I_p = 60 \text{ kA}$	64,377 m ²	85,849 m ²	89,170 m ²	
200 m $(l = 140 \text{ m}, b = 60 \text{ m})$	$I_p = 15 \text{ kA}$	10,619 m ²	21,084 m ²	22,712 m ²	1,130,973 m ²
	$I_p = 30 \text{ kA}$	26,147 m ²	42,569 m ²	45,123 m ²	
	$I_p = 60 \text{ kA}$	64,377 m ²	90,144 m ²	94,152 m ²	

EGM, electrical geometry model.

TABLE 4 The equivalent collection area predicted by the method in this study

H/m	Return stroke current/kA :	Blade angle of the wind turbine		
		0°	30°	60°
110 m ($l = 70$ m, $b = 40$ m)	$I_p = 15$ kA	36,643 m ²	42,310 m ²	46,429 m ²
	$I_p = 30$ kA	109,858 m ²	110,023 m ²	116,773 m ²
	$I_p = 60$ kA	482,749 m ²	312,591 m ²	477,663 m ²
160 m ($l = 110$ m, $b = 50$ m)	$I_p = 15$ kA	50,670 m ²	53,989 m ²	54,500 m ²
	$I_p = 30$ kA	150,673 m ²	153,907 m ²	154,634 m ²
	$I_p = 60$ kA	622,533 m ²	474,995 m ²	643,906 m ²
200 m ($l = 140$ m, $b = 60$ m)	$I_p = 15$ kA	61,575 m ²	64,939 m ²	71,164 m ²
	$I_p = 30$ kA	183,984 m ²	155,592 m ²	174,665 m ²
	$I_p = 60$ kA	766,661 m ²	547,808 m ²	690,843 m ²

trend of the results calculated by the equation of the R_s from IEC 62305-1. Observe that the data from this paper are much larger than that adopting the equation from IEC 62305-1; this is

because the striking distance from the IEC 62305-1 is failed to take into account the presence of the UPL, which is only considered a function of the I_p and assumed to be independent of the H , resulting in a smaller A_e .

Additionally, for the same I_p , the A_e of a wind turbine increases with the increase of θ employing the equation of the R_s from IEC 62305-1. And the calculation results from this paper are in accordance with the change of this trend only for a small I_p and a low H , but in response to a large return current or a high wind turbine, the wind turbine of 30° has the smallest A_e . That is, for a wind turbine of an asymmetric state like $\theta = 30^\circ$, the large shielding effect among the blades results in a much smaller striking distance of No. 3 blade, and furthermore leads to a lower A_e than that of 0° and 60°.

Likewise, the striking distance for the wind turbine at the blade angle of 60° is lower than that of 0°, and the corresponding A_e should also be reduced. On the contrary, for a low I_p , the A_e of the wind turbine of 60° is the largest due to the change of the posture for wind turbine blades. When the I_p is great, the A_e increased by the change of the posture for wind turbine blades at a blade angle of 60° is not enough to compensate for

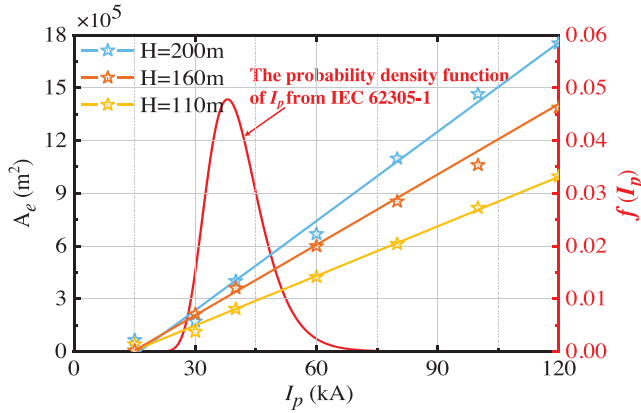


FIGURE 13 The equivalent collection area and the probability density function of I_p with different lightning currents.

the difference of the A_e changed by the R_s of the blade angle; consequently, the A_e of a wind turbine as $\theta = 0^\circ$ is the largest.

The probability of lightning damage on wind turbine depends on the lightning strike risk and the efficiency of the lightning protection system (LPS). In terms of the above analysis, when the I_p is low or the wind turbine is small, there is little difference among the A_e under different blade angles, and the difference in the probability of lightning strike accident is mainly relevant to the efficiency of LPS. Conversely, when the I_p is large or the wind turbine is tall, the effect of the blade rotation on the A_e cannot be neglected.

It is also demonstrated from the results that IEC 61400-24 standard overstates the A_e when there is a low return stroke current. Conversely, adopting the striking distance equation from the IEC 62305-1 has the disappointment of insufficient protection margin. Nevertheless, the results obtained in this paper are in the middle, which not only has a great protection margin, but also does not overstate the LPL.

4.3.2 | Analysis of the annual lightning flash number

Due to the symmetrical arrangement structure of three wind turbine blades, the A_e varies periodically six times per revolution of the wind turbine. Therefore, the average value ($A_e(I_p)$) can be calculated according to the A_e of the different blade angles obtained above. The A_e and $f(I_p)$ with different I_p is given in Figure 13, the A_{eq} and N_d can be evaluated based on the corresponding equation in Section 4.2.

According to Equation (20), it is noted that owing to the various $f(I_p)$ in different regions, the A_{eq} is also different. Generally speaking, the average intensity of the lightning current at sea is usually greater than that on land. Therefore, under the same conditions, the A_{eq} of the offshore wind turbine is also greater than that of the onshore. On the other hand, due to the stochastic nature and branched behaviour of the lightning attachment phenomenon, it is of positive significance for eval-

TABLE 5 The difference of the N_d between the observed statistics and the calculation results predicted by various methods

H/m	Method	A_{eq}	N_d	Observation data (CG-)	Difference
110 m	IEC 61400	342,119 m ²	1.02	0.5956 (Garolera)	71%
	IEC (EGM)	61,748 m ²	0.18		-70%
	Eriksson	389,255 m ²	1.16		95%
	This paper	190,270 m ²	0.57		4%
160 m	IEC 61400	723,822 m ²	2.16	0.5956 (Garolera)	263%
	IEC (EGM)	64,488 m ²	0.19		-68%
	Eriksson	823,549 m ²	2.45		311%
	This paper	264,820 m ²	0.79		32%
200 m	IEC 61400	1,130,973 m ²	3.37	0.5956 (Garolera)	466%
	IEC (EGM)	67,239 m ²	0.20		-66%
	Eriksson	1,286,796 m ²	3.83		543%
	This paper	310,670 m ²	0.93		56%

uating the lightning risk of the wind turbines to increase A_{eq} appropriately from the perspective of safety protection.

Taking the statistical analysis of wind turbines in the wind farm located in Kansas from Garolera [36] as an example, the N_d of negative cloud-to-ground flash is about 0.5956 time year⁻¹ and the N_g is 2.98 km⁻² year⁻¹. So, the N_d estimated by the various models are shown in Table 5 for N_g of 2.98 km⁻² year⁻¹ and the results of the observation statistics are compared with the estimations from the IEC standard, an alternative approach proposed by Eriksson [4] and the improved method presented in this paper. It can be observed from Table 5 that the N_d calculated from IEC 61400-24 standard and the approach proposed by Eriksson will be far larger than the statistical value for a high wind turbine. Since these two methods assume a proportional relationship between the A_{eq} and the three times and square of the H , and they do not include any physical basis but simply suppose a large area, which make it possible to generally cover the A_{eq} under any cases. However, the equivalent collection area, evaluated by the striking distance equation from the IEC 62305-1 based on EGM, underestimates the value of the N_d , which is apparently different from the observed statistics. And the N_d estimated by the improved method is 0.57, 0.79 and 0.93 for 110, 160 and 200 m high wind turbines, correspondingly. Note that there is only a difference of 4% between the calculated value (0.57 time year⁻¹, 110 m) and the observation value (0.5956 time year⁻¹) according to Garolera, with all wind turbines having a maximum total height of 125 m.

Then, to further verify the reliability of our model, the calculation results from the IEC 61400-24 [37], the Eriksson model [4], the IEC (EGM) model [34], the Rizk model [38] and the method presented in this paper are compared in Figure 14. Based on the method proposed in this paper, the quantitative relationship between the wind turbine height and the N_d is obtained. It can be observed from Figure 14 that the N_d calculated from the IEC 61400-24 standard and the Eriksson

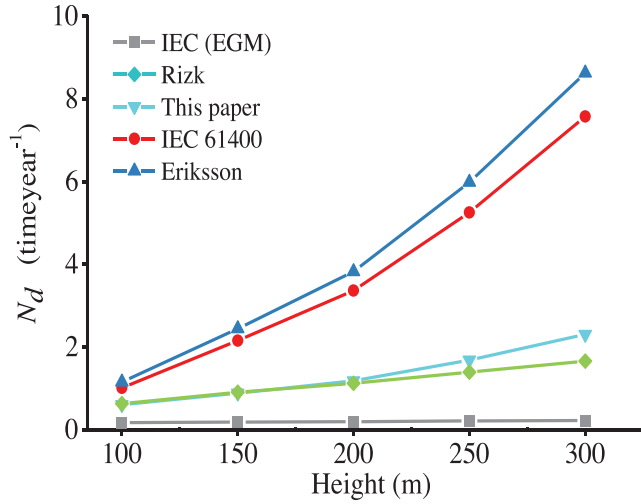


FIGURE 14 The value of the N_d calculated by the different models.

model is excessively large when the wind turbine is tall, which badly overstates the value of the N_d . Also, the N_d evaluated by the striking distance equation from the IEC 62305-1 based on EGM underestimates the value of the N_d , which has the disappointment of insufficient protection margin. These three methods are apparently different from the objective fact. By contrast, the value estimated by the Rizk model and the method proposed in this paper can better reflect the downward lightning risk of the wind turbine, which not only has a great protection margin, but also does not overstate the LPL.

4.3.3 | Classification of lightning protection levels for wind turbines

The inaccurate estimation of N_d for a wind turbine will directly lead to the error of LPLs and the deficiency of lightning protection dependability of blade LPS is caused by the design and manufacture based on the wrong LPL, which make it more vulnerable to suffer lightning damage. In terms of IEC TR 61400-24 [39], lightning protection is divided into four levels (defined as LPL) according to their maximum current: where E is the efficiency of blade LPS, E_i is the interception efficiency of the wind turbine blade, E_s is the sizing efficiency of blade LPS.

The minimum LPS efficiency can be defined by using the following equation from IEC TR 61400-24:

$$E \geq 1 - \frac{N_c}{N_d} \quad (21)$$

where N_c is the permitted annual number of critical events. The value of N_c ranges from 10^{-2} to 10^{-3} .

Therefore, the corresponding LPL can be obtained according to the calculation results of the N_d above. The N_d evaluated based on the proposed model is substituted into Equation (21) to calculate: E is 0.9824, 0.9873 and 0.9892 when the fan height is 110, 160 and 200 m, respectively. Therefore, according to

TABLE 6 The classification of lightning protection level

LPL	E_i	E_s	$E = E_i \times E_s$
I	0.99	0.99	0.98
II	0.97	0.98	0.95
III	0.91	0.97	0.90
IV	0.84	0.97	0.80

Table 6, the three wind turbines should be protected according to LPL I as $E \geq 0.98$, and an LPS with the E of 98.24%, 98.73% and 98.92% is supposed to be installed for the three wind turbines, correspondingly.

The calculation result of E is 0.9444, 0.9474 and 0.95, respectively, adopting the N_d calculated by the equation of the R_s from IEC 62305-1, so that the wind turbine of 110 and 160 m can only be classified into LPL III and 200 m into LPL II. In view of the description of different LPLs, the lightning current parameters corresponding to LPL II and LPL III are lower than LPL I. If the wrong LPL is adopted, it will inevitably increase the probability of lightning damage suffered by wind turbines. Observe also that the E obtained from the N_d calculated by IEC 61400-24 standard and Eriksson's calculation scheme is far greater than 0.99 after estimation, largely exceeding the standard of LPL I ($E \geq 0.98$). Of course, the enhancement of the LPL is of great benefit to the equipment's ability to withstand lightning damage, but oversteating the LPL required for the wind turbine can lead to excessive design and more complex manufacturing processes.

5 | CONCLUSION

In this paper, based on an improved stochastic lighting model, a new equation of the striking distance to wind turbine blades and a modified calculation method for the annual lightning flash number strikes to a wind turbine are put forward. The model employed in this paper reflects the interaction of downward and MULs and the stochastic nature of the lightning attachment phenomenon. Also, the new equation for striking distance can provide a more physically realistic basis for lightning protection analysis and the calculation method in this work can effectively reduce amount of computation directly simulated by the 3D model, which provides the guidance of calculation results for the optimization and design of the blade LPS design. The following conclusions are exhibited:

Firstly, the R_s derived from this paper is larger than the values assumed in the other methods for lightning current exceeding 40 kA or for a high-wind turbine. Besides, the striking distance of the blade tip is influenced by blade angles, while the striking distance of No. 3 blade at a blade angle of 30° is the smallest. Then, the observation data demonstrates the reliability of the equation established in this paper. The results show that the EGM does not fully satisfy the need of protection for high-wind turbines or a large lightning current.

Secondly, it can be seen from the results that the previous equation of the R_g is based on the background of transmission lines; the conclusions do not fully represent the larger distortion degree of the wind turbine to the electric field in the nearby space.

Furthermore, combined with the traditional EGM, the calculation method of the A_e and the N_d is modified. For a low I_p , the A_e for a wind turbine of 60° is largest owing to the change of the posture for wind turbine blades. When the I_p is great, the A_e of a wind turbine as $\theta = 0^\circ$ is the largest. Moreover, it is observed that the A_e is strongly overstated in the IEC 61400-24 standard. Conversely, adopting the striking distance equation from the IEC 62305-1 has the disappointment of insufficient protection margin. The results obtained in this paper are in the middle, which not only has a great protection margin, but also does not overstate the LPL.

The N_d estimated by the modified method is 0.57, 0.79 and 0.93 for 110 m, 160 and 200 m high wind turbines, correspondingly. And there is only a difference of 4% between the calculated value (0.57 time year⁻¹, 110 m) and the observation value (0.5956 time year⁻¹, 125 m) according to Garolera, with all wind turbines having a maximum total height of 125 m. The accuracy of the prediction model of lightning strike probability for wind turbine is verified.

AUTHOR CONTRIBUTIONS

Xiaoyan Bian: Conceptualization, Formal analysis, Resources, Supervision, Project administration, Writing-review & editing; **Yong Wu:** Methodology, Software, Validation, Investigation, Data curation, Writing-original draft, Visualization; **Qibin Zhou:** Validation, Formal analysis, Investigation, Resources, Writing-review & editing, Supervision, Project administration; **Ruijiao Jiang:** Methodology, Validation; **Yao Zhang:** Supervision; **Lyuwen Chen:** Supervision, Funding acquisition; **Qi Qi:** Supervision, Validation; **Weitao Lyu:** Validation, Funding acquisition, Project administration.

ACKNOWLEDGEMENTS

This work was financially supported in part by the National Key Research and Development Program of China (Grant 2017YFC1501504) and the Open Grants of the State Key Laboratory of Severe Weather (No. 2021LASW-B06).

CONFLICT OF INTEREST STATEMENT

The authors declare no conflict of interest.

DATA AVAILABILITY STATEMENT

The data that support the findings of this study are available from the corresponding author upon reasonable request.

ORCID

Yong Wu  <https://orcid.org/0000-0002-1358-6114>

REFERENCES

- Marugán, A.P., Márquez, F.P.G., Perez, J.M.P., Ruiz-Hernández, D.: A survey of artificial neural network in wind energy systems. *Appl. Energy* 228, 1822–1836 (2018)
- Wang, Y., Deng, Y., Liu, Y., Qu, L., Wen, X., Lan, L., Wang, J.: Influence of blade rotation on the lightning stroke characteristic of a wind turbine. *Wind Energy* 22(8), 1071–1085 (2019)
- Love, E.R.: Improvement on lightning stroke modelling and applications to design of EHV and UHV transmission lines. M.Sc. Theses, University of Colorado (1973)
- Eriksson, A.J.: The incidence of lightning strikes to power lines. *IEEE Trans. Power Delivery* 2(3), 859–870 (1987)
- Cooray, V., Kumar, U., Rachidi, F., Nucci, C.A.: On the possible variation of the lightning striking distance as assumed in the IEC lightning protection standard as a function of structure height. *Electr. Power Syst. Res.* 113, 79–87 (2014)
- Ioannidis, A.I., Tsovilis, T.E.: Shielding failure of high-voltage substations: A fractal-based approach for negative and positive lightning. *IEEE Trans. Ind. Appl.* 57(3), 2317–2325 (2021)
- Guo, Z., Li, Q., Ma, Y., Ren, H., Fang, Z., Chen, C., Siew, W.H.: Experimental study on lightning attachment manner to wind turbine blades with lightning protection system. *IEEE Trans. Plasma Sci.* 47(1), 635–646 (2018)
- Cooray, V., Rakov, V., Theethayi, N.: The lightning striking distance—Revisited. *J. Electrostat.* 65(5–6), 296–306 (2007)
- Armstrong, H.R., Whitehead, E.R.: Field and analytical studies of transmission line shielding. *IEEE Trans. Power Apparatus Syst.* (1), 270–281 (1968)
- IEEE Std 998–2012, IEEE Guide for Direct Lightning Stroke Shielding of Substations, Institute of Electrical and Electronics Engineers, New York (2012)
- IEEE Std 1243–1997, IEEE Guide for Improving the Lightning Performance of Transmission Lines, Institute of Electrical and Electronics Engineers, New York (1997)
- Peesapati, V., Cotton, I., Sorensen, T., Krogh, T., Kokkinos, N.: Lightning protection of wind turbines—A comparison of measured data with required protection levels. *IET Renew. Power Gener.* 5(1), 48–57 (2011)
- Long, M., Becerra, M., Thottappillil, R.: On the lightning incidence to wind farms. In: 2016 33rd International Conference on Lightning Protection (ICLP), IEEE, pp. 1–5 (2016)
- Petrov, N.I., Petrova, G.N., D'alejandro, F.: Quantification of the probability of lightning strikes to structures using a fractal approach. *IEEE Trans. Dielectr. Electr. Insul.* 10(4), 641–654 (2003)
- Jiang, R., Lyu, W., Wu, B., Qi, Q., Ma, Y., Su, Z., Wu, S., Xie, Z., Tan, Y.: Simulation of cloud-to-ground lightning strikes to structures based on an improved stochastic lightning model. *J. Atmos. Sol. Terr. Phys.* 203, 105274 (2020)
- Guo, J., Zhang, X., Wang, B., Hao, X., Zheng, S., Xie, Y.Z.: A three-dimensional direct lightning strike model for lightning protection of the substation. *IET Gener. Trans. Distrib.* 15(19), 2760–2772 (2021)
- Tan, Y., Guo, X., Zhu, J., Shi, Z., Zhang, D.: Influence on simulation accuracy of atmospheric electric field around a building by space resolution. *Atmos. Res.* 138, 301–307 (2014)
- Qi, Q., Lyu, W., Wu, B., Ma, Y., Chen, L., Liu, H.: Three-dimensional optical observations of an upward lightning triggered by positive cloud-to-ground lightning. *Atmos. Res.* 214, 275–283 (2018)
- Ioannidis, A.I., Mikropoulos, P.N., Tsovilis, T.E., Karanikiotis, N.: Fractal-based approach for modelling electric breakdown of air gaps: An application to a 75 cm positive rod-plane gap. In: The International Symposium on High Voltage Engineering, pp. 1295–1305. Springer, Cham (2019)
- Iudin, D.I., Rakov, V.A., Mareev, E.A., Iudin, F.D., Syssoev, A.A., Davydenko, S.S.: Advanced numerical model of lightning development: Application to studying the role of LPCR in determining lightning type. *J. Geophys. Res. Atmospheres* 122(12), 6416–6430 (2017)
- Mansell, E.R., MacGorman, D.R., Ziegler, C.L., Straka, J.M.: Charge structure and lightning sensitivity in a simulated multicell thunderstorm. *J. Geophys. Res. Atmospheres* 110(D12) (2005)
- Becerra, M., Cooray, V.: On the velocity of positive connecting leaders associated with negative downward lightning leaders. *Geophys. Res. Lett.* 35(2) (2008)

23. Saba, M.M.F., Paiva, A.R., Schumann, C., Ferro, M.A.S., Naccarato, K.P., Silva, J.C.O., Siqueira, F.V.C., Custódio, D.M.: Lightning attachment process to common buildings. *Geophys. Res. Lett.* 44(9), 4368–4375 (2017)
24. Guo, Z., Li, Q., Yu, W., Arif, W., Ma, Y., Siew, W.H.: Experimental study on lightning attachment manner to rotation wind turbine blade. In: 2018 34th International Conference on Lightning Protection (ICLP), pp. 1–5, IEEE (2018)
25. Srivastava, A., Mishra, M.: Positioning of lightning rods using Monte Carlo technique. *J. Electrostat.* 76, 201–207 (2015)
26. Iwashita, R., Shimosako, Y., Vasa, N.J., Yokoyama, S.: Protection efficiency of lightning rods based on Monte-Carlo method. *ICLP 2006* (2006)
27. Srivastava, A., Mishra, M.: Lightning modeling and protection zone of conducting rod using Monte Carlo technique. *Appl. Math. Modell.* 37(24), 9858–9864 (2013)
28. Mata, C.T., Rakov, V.A.: Monte Carlo modeling of lightning incidence to structures. In: *International Workshop on Electromagnetic Radiation From Lightning to Tall Structures* (2009)
29. Lu, W., Qi, Q., Ma, Y., Chen, L., Yan, X., Rakov, V.A., Wang, D., Zhang, Y.: Two basic leader connection scenarios observed in negative lightning attachment process. *High Voltage* 1(1), 11–17 (2016)
30. Tran, M.D., Rakov, V.A.: A study of the ground-attachment process in natural lightning with emphasis on its breakthrough phase. *Sci. Rep.* 7(1), 1–13 (2017)
31. Jiang, R., Qie, X., Zhang, H., Liu, M., Sun, Z., Lu, G., Wang, Z., Wang, Y.: Channel branching and zigzagging in negative cloud-to-ground lightning. *Sci. Rep.* 7(1), 1–8 (2017)
32. Petrov, N.I., Waters, R.T.: Determination of the striking distance of lightning to earthed structures. *Proc. Royal Soc. London Series A Math. Phys. Sci.* 450(1940), 589–601 (1995)
33. Eriksson, A.J.: An improved electrogeometric model for transmission line shielding analysis. *IEEE Trans. Power Delivery* 2(3), 871–886 (1987)
34. IEC 62305-1: 2010, Protection Against Lightning-Part 1: General Principles, International Electrotechnical Commission, Geneva, Switzerland (2010)
35. Saba, M.M., De Paiva, A.R., Silva, J.C.O., Silva, L.D., Noveline, C., Schumann, K.P., Naccarato, K.P.: Upward connecting leaders from buildings. In: *International Symposium on Lightning Protection (XIII SIPDA)*, Balneario Camboriu, Brazil (2015)
36. Garolera, A.C.: Lightning Protection of Flap System for Wind Turbine Blades, Technical University of Denmark (2014)
37. IEC 61400-24:2019, Wind Energy Generation Systems-Part 24: Lightning Protection; International Standard, International Electrotechnical Commission, Geneva, Switzerland (2019)
38. Rizk, F.A.: Modeling of lightning incidence to tall structures. II. Application. *IEEE Trans. Power Delivery* 9(1), 172–193 (1994)
39. IEC TR 61400-24:2002, Wind turbine generation system-Part 24: Lightning protection, International Electrotechnical Commission, Geneva, Switzerland (2002)

How to cite this article: Bian, X., Wu, Y., Zhou, Q., Jiang, R., Zhang, Y., Chen, L., Qi, Q., Lyu, W.: Quantitative characteristics of the striking distance to wind turbine blades based on an improved stochastic lightning model. *IET Gener. Transm. Distrib.* 1–14 (2023). <https://doi.org/10.1049/gtd2.12808>